Developments in the design and production of error sensitive smart coatings

Henrik Fabricius

DELTA Lys & Optik, Danish Academy of Technical Sciences
Hjortekaersvej 99, DK-2800 Lyngby, Denmark

ABSTRACT

The deposition of smart-filters like the V-lambda filter demands a precise knowledge of the refractive index at every position in the multilayered thin-film structure, and the ability to control the optical thickness of each layer precisely.

The smart-filters produced by us today are soft coated of Zinc-Sulphide (ZnS) and Misch-Fluoride (MiF). The deposition of the complex multilayered structures is controlled by a computer based system collecting data from a transmission measuring system. Special test runs have revealed that the packing density of the ZnS depends on the physical thickness of the undercoat - whereas the packing density of the MiF depends on the substrate temperature and the packing density of the undercoat. The substrate temperature that depends on the radiated heat from the crucibles, the speed of deposition and the radiation of heat to the surroundings is predictable when the thin film design is known. The speed of deposition is servo controlled and the time consumption for the coating process stays within ± 5% of the predicted value.

Key words: smart-filter, V-lambda filter, packing density, substrate-temperature, automation, Zinc-sulphide, Misch-Fluoride

1. INTRODUCTION

In recent years, new design techniques have been evolved that make it possible to design optical thin-film components with an optical performance that was very hard or impossible to obtain earlier. The so-called inverse Fourier transform method[1,2,3,4] and Tichonravov's Needle Optimization Technique[4,5] are some of these new techniques. It is for example possible to design smart-filters that can be used to correct the spectral response of sensor-systems for measurement of colour, retroreflection or luminance. The V-lambda curve describing the colour sensitivity of the human eye is a typical example of a desirable system response[2]. Unlike traditional filters designed on basis of a quarter wave stack or other regular structures, the smart-filters typically consist of layers with very different thicknesses, of which some can approach quarter-wave thickness whereas the thinnest layers are only a few nanometres thick. Obviously, these filters are a big challenge in a thin-film production[6]. Using an optical measuring system like we do, the complex code demands frequent shifts in the steering-wavelength. The thin layers demand a very stable measuring system[6], and the filters turn out to be very sensitive to fluctuations in the refractive indices and small errors in the layer thicknesses. Along with these conditions, the long lasting processing makes the steering of the deposition of the smart-filters to an exhausting and demanding task for the operator. At present, we can soft-coat the new type of filter by traditional thermal evaporation of Zinc-Sulphide (ZnS) and Misch-Fluoride[7] (MiF). We are working on transferring the technique for Ion Assisted Deposition (IAD) of hard oxide materials. However, this paper does only deal with the former work. We chose the thin-film materials ZnS and MiF because these materials have a high refractive index contrast[8], and because we have applied these materials for the production of optical filters for the visible range for more than 30 years. Unlike the high indexed oxide-materials, the ZnS (that has a bulk-index of about 2.387) already obtains a high packing density when deposited on unheated glass-substrates. The Misch-Fluoride[9] (bulk-index of around 1.384) is a high quality mixed fluoride allied to cryolite and chiolite, but is considered to form thin-films with a more homogeneous composition. According to investigations[10], paid for by us, the chemical composition of MiF lies in the range between $NaAlF_4$ and $Na_6Al_5F_{21}$.

In 1993, we succeeded in developing a computer-based system that controls and steers the deposition of our smart-filters on basis of the data from a transmission measuring system. Figure 1 is a schematic illustration of this system configured around a Balzers BAK600 coating machine. The developed system is also used for the production of a series of more traditional soft-coated filters. In contrast to an operator who operates the system manually, the computer system does only make objectively based on-line corrections. At the same time, the system is capable of extracting the speed of deposition from the optical measurement and servo controlling the speed of deposition. An immediate effect was an improved uniformity of the filters from different productions. In this way it was made visible that the deviations between the predicted and the actual variations of the measuring signals were very systematic. Concerning the smart-filters, the steering problems resulted in distinct and systematic discrepancies in spectral performance of the finished filters (see figure 2). Calculations on the computer made us suspect that the

0-8194-2161-8/96/$6.00

problem was variations in the packing densities of the layers.

2. A METHOD FOR THE DETERMINATION OF THE PROGRESS OF THE REFRACTIVE INDEX IN MULTI-LAYERED STRUCTURES

Everyone who has tried to control the deposition of a classical soft-coated bandpass-filter on basis of the signals from an optical measuring system knows that the variation of the transmission (T_{min}/ T_{max}) at a fixed wavelength is nearly constant during the deposition of each of the resonating layers. The signal may drift with the temperature of the substrates, but the modulation of the transmission is nearly constant. Therefore, I believe that the most distinct changes in the packing density are going on when switching materials.

One way it is possible to form a general view of which variations is going on in the multilayered structure is to deposit a three-quarter-wave stack and back trace it to determine the refractive index in the different layers. Despite minor errors in the thicknesses of the layers, each layer will give you three turning points at the measuring curve and calculating the refractive index of the layer on basis of these data is always possible. Our system performs on-line mathematical fits on the measuring data, and the tolerance on the transmission measurement at the turning points is less than 0.01%. Given the bulk index n_B, the packing densities of the different layers are calculated by the following equation[11,12]

$$P = \frac{n_B^2 + 2}{n_B^2 - 1}\,\frac{n^2 - 1}{n^2 + 2} \qquad (1)$$

Figures 3 and 4 show the variations of the packing densities as function of the thickness of the thin-film when the materials are deposited on unheated substrates in our BAK600 system. The temperature measurement done on a dummy substrate placed next to the rotating substrate holder was progressing as shown in figure 5.

Figures 6, 7 and 8 show correspondently the variations of the packing densities as function of the thickness of the thin-film when the test-structure is deposited on glass-substrates preheated to a temperature of 105°C with a 1000W iodine quartz lamp.

Comparing the figures 3 and 6, it is seen that the packing density of the ZnS layers seems independent of the substrate temperature in the investigated range. However, it is clearly seen from the rest of the figures that the packing density of the MiF layers increases remarkably with the temperature - a characteristic that is typical when deposing fluorides[11,12,13,14,15].

For economical, time, and yield-concerning reasons, we normally prefer to deposit the thin-films on unheated substrates. This means that we have much interest in developing a model by means of which we may predict the temperature of the substrates and the packing density in the temperature sensitive MiF layers. In the following, we will try to develop such a model. We will assume that the temperature we measure on the dummy substrate is equal to the temperature of the centre substrate in the rotating substrate holder. This is not necessarily the case, but we believe that they are closely related. Furthermore, it is important to comprehend that the basis of this work is the known packing densities of the layers in the test-coatings and the temperatures that we measured at the dummy substrate with a chromel-alumel thermometer.

3. MODEL FOR THE PREDICTION OF THE PROGRESS OF THE SUBSTRATE-TEMPERATURE

The deposition is carried out at a pressure of less than 10^{-5}mBarr, and the amount of material deposited is small compared with the mass of substrates. This means that the substrates are mainly heated by the infrared radiation from the hot sources that consist of a flat-bottomed alumina-oxide crucible containing the thin-film material and a tungsten coil with a certain resistivity placed directly above the crucible. Coatings for the visible spectral range typically transmit fully in the wavelength-range above 2.4 μm where the glass-substrate begins to absorb. Therefore, we neglect the influence of the coating on the heat transfer. Designating the voltage across the tungsten coil with V(t), the substrates receive the energy

$$E_{in}(t) = c_1 \int_{to}^{t} V^2(u)\, du \qquad (2)$$

where t is the time and c_1 a constant. However, according to Stefan-Boltzmann's law some of the energy is reradiated from the substrates that have the temperature $T_s(t)$ to the surroundings that have a temperature of $T_v(t)$ (cold walls of the chamber)

$$E_{out}(t) = c_2 \int_{to}^{t} T_s^4(u) - T_v^4(u)\, du \quad (3)$$

where c_2 is a constant. The substrate temperature, $T_s(t)$, changes gradually as expressed by

$$T_s(t) - T_s(t_0) = (E_{in}(t) - E_{out}(t))/C_s \quad (4)$$

where C_s is the heat capacity of the substrates. Concerning the time, t, we must expect that the temperature will be

$$T_s(t) = D \int_{to}^{t} V^2(u)\, du - B \int_{to}^{t} T_s^4(u) - T_v^4(u)\, du + T_s(t_0) \quad (5)$$

The coefficients B and D were determined on basis of data from the two types of test-runs. The thin curves in figure 9 show the measured progress of the temperature, and the thick curves show the obtained estimates. For comparison, figure 10 shows the measured and the estimated progress of the temperature for one of our smart-filter depositions, when the same B and D values are applied. It appears from figures 9 and 10 and the experience from the subsequent productions that the estimate of the temperature typically fits within 5 degrees. At temperatures beyond 100°C, there is a clear tendency that the temperature estimate is too high. However, according to figure 4 this is of minor importance, as our main interest is to use the estimate of the temperature to obtain a prediction of the packing density in the MiF layers.

4. ESTIMATION OF THE PROGRESS OF THE TEMPERATURE FOR A KNOWN FILTER-DESIGN

If we wish to predict the progress of the temperature during the deposition of a certain multi-layered structure, we need a precise knowledge about the involved times and the increasing power consumption during the deposition-process. When the computer controlled system runs the deposition of a coating, the following typical times are present

t_{start} is the time the system uses to move from the point where it has finished the deposition of one layer to the point where it is ready to deposit the following. It can be that the system must scan a monochromator, change the sensitivity of a lock in amplifier, or alter the voltage for a photo multiplier.

$t_{preheat}$ is the time it takes from we start to heat the material in the crucible until it begins to evaporate.

t_{coat} is the time it takes to deposit the layer when the source is evaporating.

t_{stop} is the time it takes to finish the deposition of a layer with precision.

The equipment applies an extra heating coil in the intervals between the different layers to minimize drifting in the optical measuring system at large optical thicknesses of the coating.

On basis of data collected from a number of productions controlled by the computer system, it was easy to describe t_{start} as function of the optical thickness, $t_{preheat}$ as function of the respective consumptions of materials, and t_{stop} as a typical time. Left is therefore first of all to describe t_{coat} as function of the thickness of each layer, the desired rate of deposition and the necessary power supply during the deposition.

4.1 Relation between the thickness of the deposited thin-film and the supply of power

It was mentioned that the computer controlled system servo-controls the speed of deposition. The speed is extracted from the time dependant variation in the optical measuring signal at fixed positions in the filter structure, and the computer corrects the voltage across the heating coil when deviations from the desired rate are detected. Figure 11 shows how the computer chose to regulate V^2 as function of the deposited thickness of MiF (physical thickness) during different test-runs. The power for the heating coil must evidently be increased linearly proportional to the consumption of material from the crucible. It turns out that this is also the case when the ZnS is evaporated. However, we notice that the power consumption is a little different from run to

run, and this does of course influence the progress of the temperature. To control the progress of the temperature as good as possible, it is important to be careful when the crucibles are loaded with material, and to take care that the quality of the thin-film materials is the same from delivery to delivery.

4.2 Speed of deposition

The material is evaporated from an Al_2O_3 crucible by supplying power from a heating coil placed just above the crucible. The evaporation is not starting abruptly. It would be more correct to describe the rate of the evaporation as

$$R_j(t_j) = R_{jf}\,(1 - e^{-t_j/\tau}) \tag{6}$$

where

$$t_j = t - t_{j0} \geq 0 \tag{7}$$

where t_{j0} is the moment where the source starts to evaporate for layer number, j, and where R_{jf} is the speed of deposition the source is stabilising itself at for $t_j >> \tau$. The speed of deposition is here the change in optical thickness per time-unit at the wavelength $\lambda = 0.6\mu m$. The averages rate of evaporation $\mathbf{R_j}$ is

$$\mathbf{R_j} = R_{jf}/t_j \int_0^{t_j} (1 - e^{-t/\tau})\,dt = R_{jf}\,[1 - (1 - e^{-t_j/\tau})\tau/t_j\,] \tag{8}$$

during the deposition of the layer indexed j. The time-constant, τ, can be determined on basis of data on the average rate, and the time-consumption for the deposition of layers of sufficient different thickness where R_j is as equal as possible

$$R_{jf} = R_{if} \;\wedge\; t_j > t_i \gg \tau \;\Rightarrow\; \tau = (\mathbf{R_j}/\mathbf{R_i} - 1)/(1/t_i - 1/t_j) \tag{9}$$

When τ has been calculated, R_{jf} can be calculated and controlled for concordance by equation (8). The investigations have shown that we have the following average relation between τ and R_{jf} for the applied source-system:

$$\tau \approx 400 \cdot R_f/\mu m - 12.2/min. \tag{10}$$

The duration of the deposition of layer, j, that have a thickness of S_j, is calculated by an iterative solvation of the transcendental equation

$$t_j + \tau\, e^{-t_j/\tau} = \tau + S_j/R_{jf} \tag{11}$$

For the selected equipment, $R_{jf} = 0.033\mu m/min.$, gave an uncertainty of ± 2.5% on the total duration of the deposition of a number of filters with very different layer thicknesses. The productions we have made since have shown that the deviations in the total duration sometimes increases to ± 5%.

4.3 Estimation of the progress of the temperature for a filter-design

It is now possible to estimate the progress of the temperature during the deposition of a given filter by combining our knowledge about, how much time each operation in the deposition process consumes (e.g. see equation (11) and part 4), and how much power we have to supply to obtain the desired speed of deposition (see figure 11) with our knowledge about how the temperature changes with the supplied and radiated energy (see equation (5)). A large number of production-runs with the automatic system have proved that the estimate of the temperature is still correct within about 5 degrees.

The obtained knowledge about the progress of the temperature during the deposition can be used in different ways:
- It can be used to estimate how the spectral characteristic for a coating shifts with the temperature as the result of the thermal expansion of the materials and changes in the refractive indices of the layers. For example, a steep transition in the visible range shifts about 1 - 2nm[16] when the temperature changes 100°C and the transmission in the measuring system is altered because of this.
- The estimated temperature can also be used to estimate the resulting packing density in the temperature sensitive fluoride-layers, if we manage to determine a suitable generalized relation between these quantities, and that is what we will try to do in the following.

5. ESTIMATION OF THE PROGRESS IN THE PACKING DENSITY FOR A KNOWN FILTER-DESIGN

We will now return to the above mentioned test-runs, where we deposited a three-quarter wave stack on respectively cold and preheated substrates (designing-wavelength = 584nm, and steering-wavelength = 550nm).

5.1 ZnS

Comparing the figures 3, 5, 6 and 8, it is seen that the packing density of the ZnS-layers does not seem to depend on the temperature in the investigated temperature range. The packing density of the ZnS-layers seems not to depend much on the packing density of the underlying fluoride layers either, as this is very different in the two types of test-runs. The explanation is certainly that the ZnS is formed by a reaction between free zinc and sulphur atoms. The decrease from the first to the second data-point at the curves in figures 3 and 6 seems, however, clearly to be because the first ZnS-layer is deposited on the glass-substrate whereas the following layers are deposited on MiF-layers. We furthermore observe a slight decrease in the packing density throughout the deposition process as such. This slight decrease could in principle be the result of a certain reduction going on when switching material. However, this prediction is not confirmed when it is applied in general in computer-simulations (more about this in part 6). Different types of coatings with a larger number of layers and frequent shifts in materials did only support the theory that the packing density of each new ZnS layer seems to decrease linearly proportional to the total physical thickness of the underlying multi-layer (see figure 12). The packing density is as high as 99.4%, when the ZnS is deposited directly on glass. But it decreases about 2% immediately after the first intermediate fluoride-layer, and subsequently about 0.6% per μm in physical thickness of the underlying multi-layer.

$$P_H(t_f = 0) = 0.9941 \tag{12}$$

$$P_H(t_f > 0) = 0.9753 - 0.0059\, t_f \ \mu m^{-1} \tag{13}$$

where t_f is the physical thickness of the underlying thin-film.

5.2 MiF

An analysis[10] has shown that MiF is a mixture of NaF and AlF_3 with a composition in the range between $NaAlF_4$ and $Na_6Al_5F_{15}$. When the MiF was deposited directly on unheated glass-substrates the average packing density was determined to be 87.8%, assuming that the bulk-index is approximately 1.384 at 550nm[7]. We did not try to deposit MiF directly on preheated substrates. But H. Pulker et al. found the following nearly linear relation between the packing density and the substrate temperature T_S in the range from 30 to 100°C for the related material cryolite[12]

$$P_L(0, T_S) \approx 0.888 + (0.925 - 0.888)/(373K - 303K) \bullet (T_S - 303K) \tag{14}$$

However, at 190°C the packing density was still referred to be equal to the one at 100°C[12].

It is evident from the figures 4 and 7, that the packing density is lower in MiF-layers deposited on top of a ZnS-layer. Comparing with figure 9, a close relation obviously exists between the progress of the temperature and the packing density of

the MiF-layers at the beginning of the multi-layer. At the end of the deposition the temperature and the packing density is nearly the same for both types of test-runs. However, it appears from figure 7 that we do not reach as high a packing density as we had when we started the deposition on the preheated substrates. We assume that this is because the MiF film (formed by combination of whole molecules[13]) both is sensitive to the temperature and to the structure of the underlying layer. It appears that subsequent to m shifts of the materials, the packing density can be described by the equation

$$P_L(m, T_{Sm}) = \alpha \bullet P_L(1, T_{Sm}) \bullet P_H(t_{f\ m-1}) \tag{15}$$

where T_{Sm} symbolises the temperature of the substrates at the beginning of the deposition after the m.th shift of the materials (m > 0), where $P_H(t_{f\ m-1})$ is given by equations (12) and (13) and where α is the constant

$$\alpha = 1/P_H(0) = 1/0.9941 \tag{16}$$

This means that $P_L(1, T_{sm})$ becomes equal to the packing density of the first MiF-layer that grows on a ZnS-layer. The progress of $P_L(1, T_{sm})$ can be evaluated by plotting $P_L(m, T_{Sm})\ P_H(0)/\ P_H(t_{f\ m-1})$ as function of the estimated temperature of the substrates during the two types of test-runs. Figure 13 is such a plot of data from the two types of test-runs and it is seen that $P_L(1, T_{sm})$ can be approximated by a polynomial of the third degree

$$P_L(1, T_{sm}) = AT_{sm}^3 + BT_{sm}^2 + CT_{sm} + D \tag{17}$$

where the coefficients A, B, C, D are

$$A = 2.257511 \bullet 10^{-7} K^{-3}$$

$$B = -2.48225 \bullet 10^{-4} K^{-2}$$

$$C = 9.1350 \bullet 10^{-2} K^{-1}$$

$$D = -10.3888 \tag{18}$$

It is noticed that the curve has a tendency to flatten out at high temperatures and that the initial slope of the curve is larger than expressed by equation (14). This means that the fluoride-layers are more sensitive to the substrate-temperature when they are part of a multi-layer than when they are deposited directly on a glass-substrate.

The thick curves in figure 14 shows a combined plot of the progress of the packing density of the MiF-layers as estimated by equation (15) for the two types of test-runs (see figures 4 and 7). The thin curves are the corresponding plots of the measured packing densities. Equation (15) obviously seems to be fulfilled.

5.2.1 Entrance-zone

It is well-known that there has been observed inhomogeneities in the refractive index of many fluoride-films[12,17,18]. However, this effect is weak compared with the variations observed in this paper. Furthermore, the properties of MiF are believed to be superior to those of cryolite and chiolite in this respect. Therefore, we normally assume that the refractive index is constant in each layer. However, the first MiF-layer in the multi-layer is an exception, when it is deposited on unheated substrates. Computer simulations have revealed that the packing density is extraordinarily low in the first 26 nm of this layer. A reduction of the refractive index in this zone of about 1% seems appropriate.

6. GENERALISATION OF THE DERIVED RESULTS

It is evident from the equations (12), (13) and (15) that the application of the derived model describing the variations in the packing density of the layers seems not to be especially connected to the selected test coatings.
- The packing density of ZnS-layers deposited on top of MiF-layers seems only to depend on the total physical thickness of the underlying multi-layer.
- The packing density of the MiF-layers seems on the opposite to be determined by the packing density of the underlying ZnS-layer and by the temperature of the multi-layer when the MiF-layer is initialised.

The fact that we have a computer controlled deposition system at our disposal that always conducts a regular steering of the deposition process and collects the measuring data continuously, is of big advantage when we want to test the general applicability of the derived model. It gives us the possibility to software simulate the whole process of deposition and to test the derived models that describe the packing-conditions on a lot of different filters with different compositions. This type of investigation has established that it is possible with advantage to transfer the results from the test-runs to describe the variations that occur in the packing conditions in coatings that consist of layers with another thickness, including smart-coatings.

The application of the model, for prediction of the substrate temperature and the resulting packing densities in the layers in a certain thin-film structure composed of ZnS and MiF, did actually make the obtained results agree better with the predictions, and the applicability of the computer controlled coating system was increased. Figure 15 gives an impression of the obtained correlation between theory and praxis for one of our V-lambda filters. When compared with figure 2, the correlation has evidently been improved. When the filters are used with a 1mm thick BG40 coloured glass and a silicon photo-diode, the so-called F1-error of the luminance-measuring system[19] is reduced from 7.6% ± 1.4% to 3.3% ± 0.5%. That is a 230% reduction.

7. CONCLUSION

It was shown that it is possible to extract equations describing the progress of the temperature and the packing density during the deposition of thin film structures composed of thermally evaporated ZnS and MiF. In the paper the following questions were discussed:

A model was derived that describes the relation between the consumption of power and time and the progress of the substrate temperature during the deposition.

Data were presented that show the relation between the consumption of material from the crucible and the power that must be supplied to maintain the desired speed of deposition.

A model was established that shows the relation between the time used to heat the thin-film material and the increase in the speed of deposition.

It is possible to estimate the total duration of the deposition of filters with very different layer-codes with a maximal margin of about ±5%

It was shown that is possible currently to estimate the substrate-temperature with a margin of about 5 degrees on basis of the layer-code and the desired speed of deposition.

It was argued that the packing density of the ZnS-layers seems only to depend on the thickness of the underlaying thin-film structure in the investigated range of temperature and thickness.

It was correspondingly argued that the packing density of the MiF layers is only determined by the packing density of the underlaying ZnS-layer and the temperature of the substrate at the beginning of the layer.

It was shown that it is possible to describe the relation between the packing density of the first MiF-layer and the substrate temperature by application of a polynomial of the third degree.

Finally, it was shown that it is possible to apply the derived model to obtain an improved correspondence between the desired and the obtained transmission curve for complicated filter-structures composed of many layers with large differences in the layer-thicknesses.

REFERENCES

1. J. A. Dobrowolski and D. Lowe, "Optical thin film synthesis program based on the use of Fourier transforms, " Appl. Opt. **17**, p. 3039 - 3050 (1978)
2. Henrik Fabricius, "Closed loop optimization of quasi-inhomogeneous optical coatings," SPIE Vol. 2046, *Inhomogeneous and Quasi-Inhomogeneous Optical Coatings*, p. 156 - 166 (1993)
3. B. G. Bovard, "Rugate filter theory: an overview," Appl. Opt. **32**, p. 5427 - 5442 (1993)
4. A. Tikhonravov , "Some theoretical aspects of thin-film optics and their applications," Appl. Opt. **32**, p. 5417 - 5426 (1993)
5. Sh. A. Furman and A. V. Tikhonravov, *Optics of multilayer systems* (Editions Frontieres, Gif-sur-Yvette, 1992), chap. 2
6. H.A. MacLeod, *Thin-Film Optical Filters* (Hilger, London, 1986) p. 424 - 432
7. Product informations on AWS II Misch-Fluorid from Dr. Hugo Anders, Optische Laboratorium, Ges. für Dünne Schichten mBH, Schwarzacher Straße 27, D-92507 Nabburg, Germany
8. H.A. MacLeod, *Thin-Film Optical Filters* (Hilger, London, 1986) p. 390 - 391
9. Paul Klocek, *Handbook of infrared optical materials*, (Marcel Dekker, Inc., New York 1991) p. 406 - 408
10. Analysis performed by the Institute of Physics at the University of Aarhus, DK-8000 Aarhus, Denmark
11. H. K. Pulker, *Coatings on glass*, (Thin films science and technology, 6, Elsevier) p. 368 - 369 (1984)
12. H. Pulker and Elmar Ritter, "Optische Eigenschaften und Struktur von Fluorid-Aufdampfschichten," *Ergebnisse der Hochvakuumtechnik und der Physik dünner Schichten*, Band II (Wissenschaftliche Verlagsgesellschaft mbH, Stuttgart), p. 244 -260 (1971)
13. E. Bauer, "Struktur und Wachstum dünner Fluorid-Aufdampfschichten," *Ergebnisse der Hochvakuumtechnik und der Physik dünner Schichten*, (Wissenschaftliche Verlagsgesellschaft mbH, Stuttgart), p. 39 - 48 (1957)
14. H.A. MacLeod, *Thin-Film Optical Filters* (Hilger, London, 1986) p. 322 - 331
15. H.A. MacLeod, *Thin-Film Optical Filters* (Hilger, London, 1986) p. 398 - 407
16. H.A. MacLeod, *Thin-Film Optical Filters* (Hilger, London, 1986) p. 310
17. S. Ogura, *Some features of the behaviour of optical thin films* (Department of Physics and Physical Electronics, Newcastle upon Tyne Polytechnic) p. 113 - 115 (1975)
18. H.A. MacLeod, *Thin-Film Optical Filters* (Hilger, London, 1986) p. 381
19. Publication CIE No 69 (1987), *Methods of Characterizing Illuminance Meters and Luminance Meters*

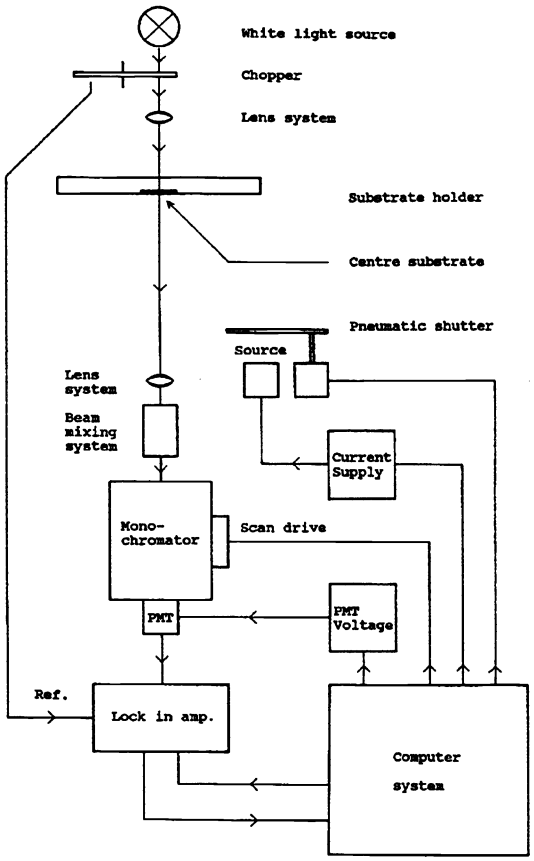

Figure 1. Schematic illustration of the developed computer controlled system. The computer collects data from the optical measuring system and controls the coating process on basis of these data.

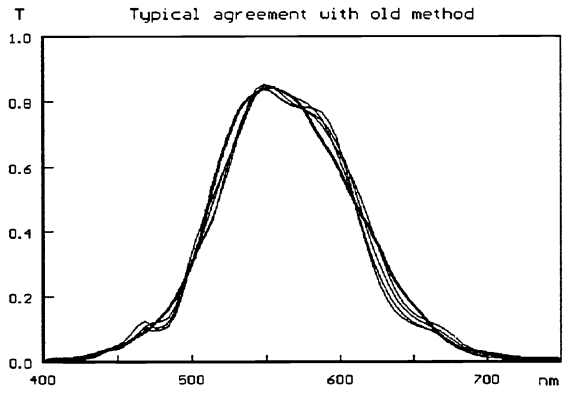

Figure 2. Thick solid curve showing the desired transmission curve of a smart-filter that gives a detector system a V-Lambda response. The thin solid curves show some obtained transmission curves.
The systematic deviations are due to differences in the packing densities of the layers that were not taken into account in the designing process.

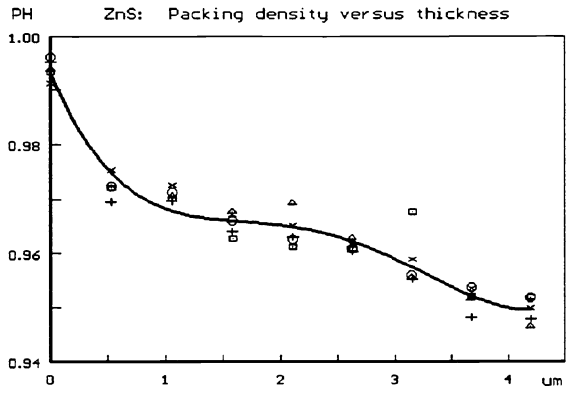

Figure 3. Packing density of the ZnS layers as function of the position in the test-coatings deposited on unheated glass-substrates

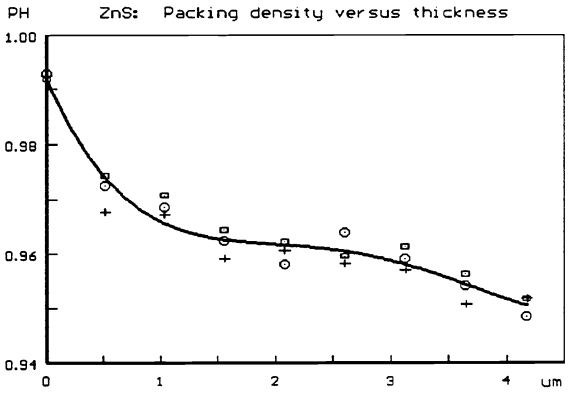

Figure 6. Packing density of the ZnS layers as function of the position in the test-coatings deposited on glass substrates preheated to 105°C.

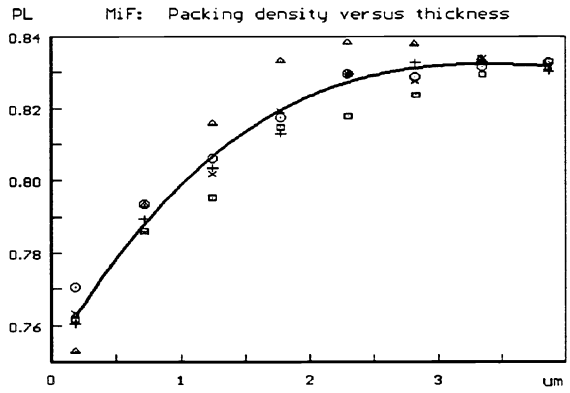

Figure 4. Packing density of the MiF layers as function of the position in the test-coatings deposited on unheated glass-substrates.

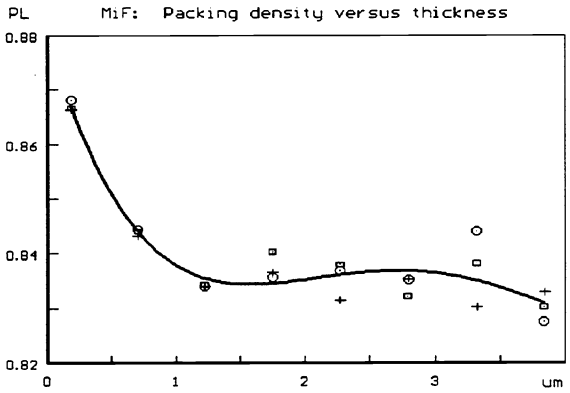

Figure 7. Packing density of the MiF layers as function of the position in the test-coatings deposited on glass-substrates preheated to 105°C.

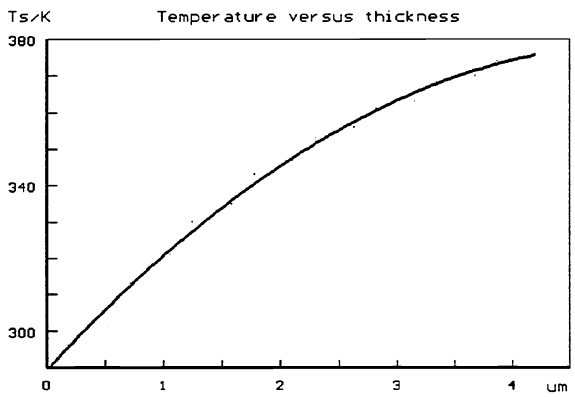

Figure 5. Temperature of substrates for test-runs where they not were preheated.

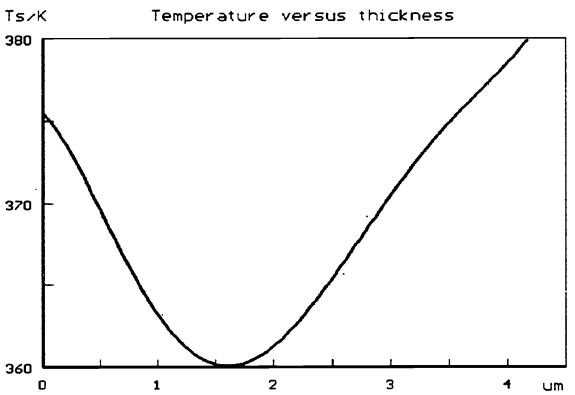

Figure 8. Temperature of substrates for test-runs where they were preheated to 105°C.

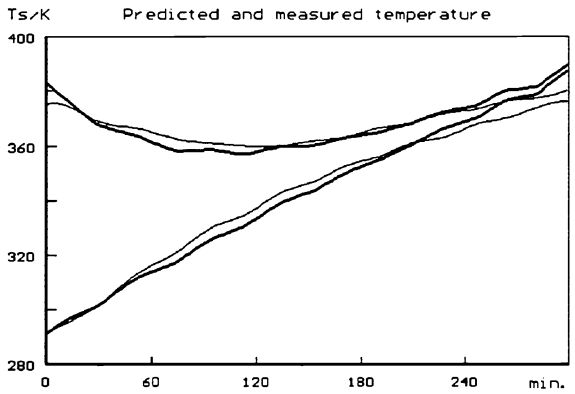

Figure 9. Thick solid curves show the obtained estimates of the changing temperature of the substrates during the two different test-runs. The thin solid curves show the corresponding measured temperatures.

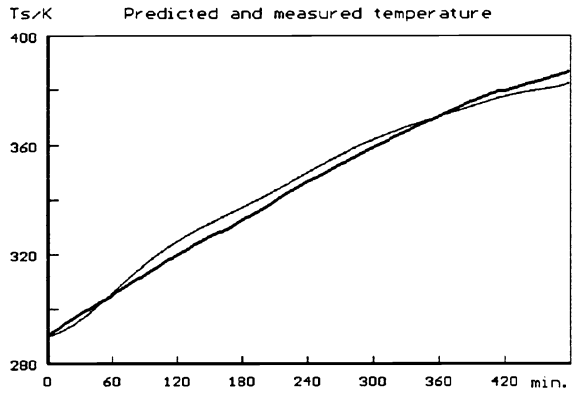

Figure 10. Thin solid line shows the measured temperatures during the deposition of a smart-filter. The thick solid line shows the corresponding estimate of the temperatures.

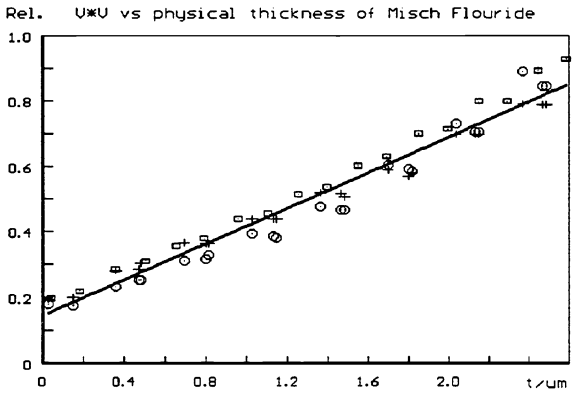

Figure 11. Plot of the power that was applied to evaporate the MiF at the desired rate during the test-runs as function of the physical thickness of the deposited MiF.

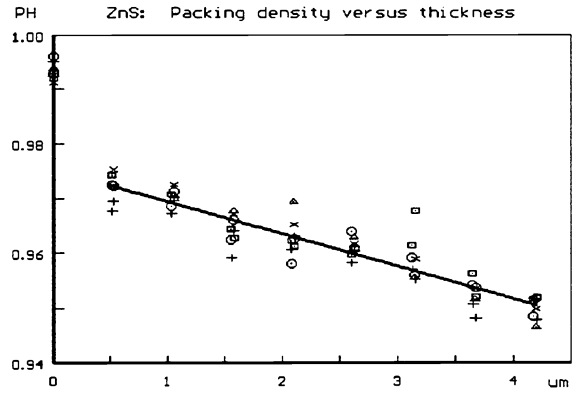

Figure 12. Packing density drops approximately 2% when deposited on a MiF-layer instead of on the glass substrate. The packing density furthermore drops linearly proportional to the thickness of the undercoat.

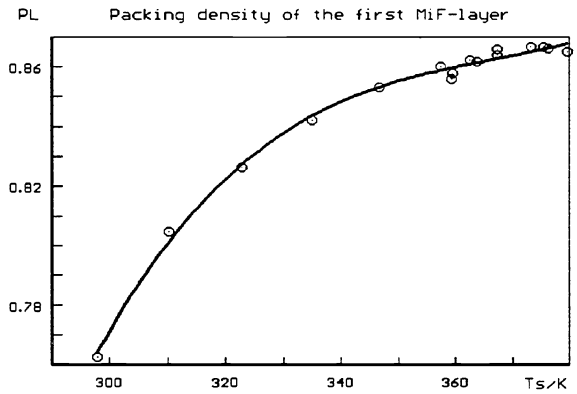

Figure 13. Packing density of the first MiF layer deposited on top of a ZnS layer, as function of the temperature of the substrates during the two different types of test-runs.

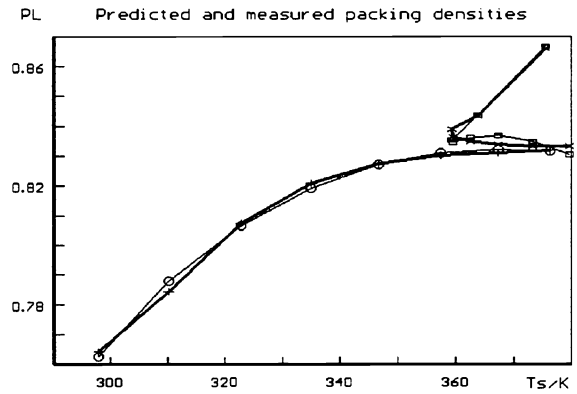

Figure 14. Thin solid curves show the packing densities of the MiF layers in the two types of test-runs as function of the respective predicted temperatures. The thick solid curves show the corresponding estimated values.

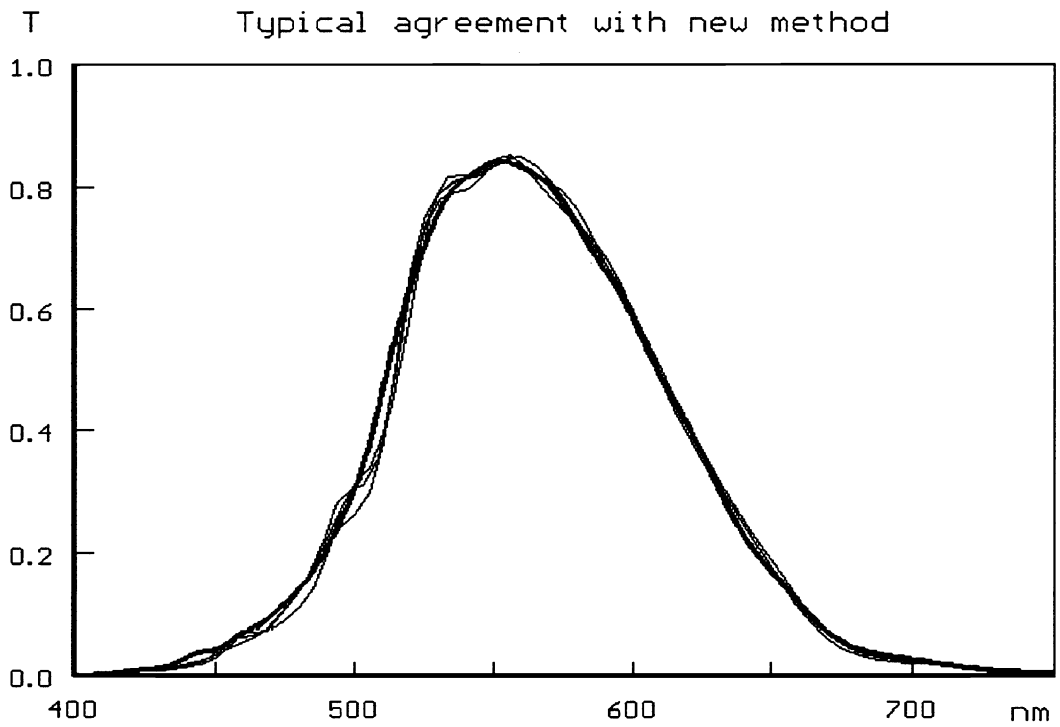

Figure 15. Thick solid curve shows the desired transmission curve of a smart-filter that gives a silicon photodiode a V-Lambda reponse when used with a 1mm thick BG40 coloured glass. The thin solid curves show some of the obtained transmission curves for the new design where the differences in the packing densities of the different layers is taken into account. The F1-error of the system that is simulating the spectral sensitivity of the human eye is 3.3% ± 0.5%.